Journal of
Applied Crystallography
ISSN 0021-8898

Received 22 January 2010
Accepted 22 September 2010

Determination of the β-quartz hexagonal cell parameters from a 00.1 neutron multiple diffraction *Umweganregung* pattern measured at 1003 K

Luiz Carlos de Campos,[a] Carlos Benedicto Ramos Parente[b]* and Vera Lucia Mazzocchi[b]

[a]Pontifícia Universidade Católica de São Paulo (PUC/SP), São Paulo, SP, Brazil, and [b]Instituto de Pesquisas Energéticas e Nucleares (IPEN-CNEN/SP), São Paulo, SP, Brazil. Correspondence e-mail: cparente@ipen.br

The hexagonal cell parameters a and c of β-quartz have been determined from a 00.1 β-quartz neutron multiple diffraction *Umweganregung* pattern measured at 1003 K. Owing to the high density of multiple diffraction peaks in the indexing of the pattern, contrasting with the low density of experimental peaks, a procedure to correctly index peaks has first been applied. After the correct indexing, the peaks were selected taking into account their quality (adequate intensity and definition) and then classified in accordance with their suitability for the determination of a or c. The azimuthal angular positions of classified peaks were applied to indexing diagrams in order to obtain sets of values for both a and c. Weighted means of the sets give final values for a and c. In order to obtain more reliable final values an iterative process has been employed. A statistical analysis of data has also been employed to calculate uncertainties for the mean values found in the iterative process. After 12 cycles of iteration, the results converged to a = 4.9957 (14) and c = 5.46184 (35) Å for β-quartz at 1003 K.

1. Introduction

Utilization of the multiple diffraction phenomenon for the determination of cell parameters has been studied by several authors. Kossel (1936) realized that some dim lines appearing in a photograph obtained by the divergent beam method could be explained as an effect of several scattered beams occurring simultaneously. Kossel suggested that the phenomenon could be used for the determination of lattice parameters. In the following year, Renninger (1937), using Cu $K\alpha$ radiation, positioned a diamond crystal in a diffractometer in such a way that a diffracted intensity if produced by the 222 forbidden reflection of diamond (nowadays this reflection is known to be almost forbidden) could be measured. Of course, no (noticeable) diffracted intensity was observed. He next turned the crystal around the scattering vector of the 222 reflection and observed the appearance of peaks, at different azimuthal angular positions, above the expected background level measured by the detector. This Renninger effect was called *Umweganregung* (*Umweg* for short). Another effect observed by Renninger was a variation in the intensity of permitted reflections in diamond and common salt (NaCl) as an increase or decrease of intensity. This effect was called *Aufhellung*. Both *Umweg* and *Aufhellung* effects belong to the same phenomenon, nowadays called multiple diffraction. Renninger, using the diffractometer method, became the first researcher to produce multiple diffraction in a systematic way. He used the azimuthal angular positions (φ positions hereinafter) of a few peaks of the 222 *Umweg* pattern to determine the cubic lattice parameter of diamond, obtaining a = 3.5594 Å with a precision of $\sim 10^{-4}$ Å. Post (1975) observed that the Renninger effect could be used to determine lattice parameters with a high accuracy. According to Post, use of multiple diffraction is advantageous since it permits the utilization of a large number of secondary reflections measured during a rotation of the crystal around the scattering vector of a primary reflection. More recently, Mazzocchi & Parente (1998) determined the cubic parameter of the ferri- and paramagnetic phases of magnetite as a by-product of the refinement of parameters in the corresponding neutron multiple diffraction (NMD) patterns.

Concerning determination of lattice parameters by using multiple diffraction, as far as we know, work done until now has treated simpler cases involving cubic lattice parameters. An exception is the work of Caticha-Ellis (1975), who made a theoretical study of the sensitivity of the multiple diffraction phenomenon when applied to determination of lattice parameters in the general case, giving emphasis to the cubic case. The present work deals with determination of the hexagonal cell parameters of β-quartz (Dana & Dana, 1962) using an NMD pattern. We used the 00.1 β-quartz NMD *Umweg* pattern measured by Mazzocchi (1984) on the IPEN multipurpose neutron diffractometer at 1003 K. This pattern is presented in Fig. 1, referred to both the experimental and the

indexing scales. It is worth mentioning that indexing of the pattern of Fig. 1 showed a high density of secondary reflections (Mazzocchi, 1984; Mazzocchi & Parente, 1994). A high density of secondary reflections, at first sight, seems to be incompatible with the observed low density of peaks in the experimental pattern. Fig. 2 illustrates this apparent dichotomy. This figure shows a small part of the experimental pattern referred only to the indexing scale. Vertical dashes above the pattern correspond to the results of the indexing. They indicate the φ positions where the secondary beams, produced by those reflections permitted by the β-quartz space group, attain their maximum intensities. Actually, for reasons of symmetry, in a 00.1 β-quartz multiple diffraction pattern secondary reflections always occur in pairs $hkl/h\,k\,(1-l)$ (Cardoso, 1983). For the sake of clarity, the Bravais–Miller indices of the pairs were omitted from Fig. 2.

Observing Fig. 2 one notes that the number of pairs is far greater than the number of peaks. This fact brought a first difficulty: how to correlate an experimental peak to the pair that is effectively responsible for its formation. In §3 it is shown how this difficulty has been overcome.

2. Experimental

To measure the 00.1 β-quartz NMD pattern of Fig. 1, Mazzocchi (1984) used a natural quartz crystal shaped into a cylinder of size 5 cm diameter × 5 cm height with the direction [00.1] approximately parallel to the cylinder axis. An experimental arrangement appropriate to NMD measurements was assembled at the IPEN neutron diffractometer. To obtain patterns with good resolution a special collimator was used. This is an evolution of the collimator conceived by Parente & Caticha-Ellis (1974). A description of the experimental arrangement as well as the special collimator is given by Mazzocchi (1984) and, with fewer details, by Mazzocchi & Parente (1994).

To heat the crystal in order to reach the β phase of quartz an electrical furnace was used. A proportional temperature controller (±3 K) controlled the temperature *via* a thermocouple placed close to the heating resistance. The crystal temperature was monitored by another thermocouple leaning on the round crystal surface. Both temperatures were registered by a two-pen register (Mazzocchi, 1984; Mazzocchi & Parente, 1994). As pointed out by Mazzocchi (1984), no significant variations in the crystal temperature were observed during the experiment.

Orientation of the quartz crystal in the neutron beam was carried out only for the primary reflection. In general, the orientation of the mirror, which is assumed as the origin in the indexing (see §3), is easily found when comparing the experimental pattern with the results of the indexing. Note in Fig. 1 that the crystal was rotated in a direction opposite that assumed in the indexing.

3. Indexing of peaks

To index the pattern of Fig. 1, Mazzocchi (1984) employed a computer program that determines the φ positions where the secondary beams attain maximum intensities. This program received no name in the Mazzocchi's work. For use in the present work a few modifications were introduced in the input and output routines and the program was named *INDEXHEX* (Campos, 2002). It is based on the geometry of a multiple diffraction experiment (Cole *et al.*, 1962). One of the symmetry mirrors occurring in a multiple diffraction pattern (Chang, 1984) is taken as the origin of the indexing scale. In this work, the symmetry mirror located approximately at 10° in the experimental scale was arbitrarily assumed as the mirror M = 120°. It corresponds to one of the six possible [10.0] directions orthogonal to the sixfold axis [00.1] in β-quartz. Indexing is done considering all secondary reflections permitted by the space group of β-quartz. However, this fact alone does not guarantee that a peak will be formed in every φ position indicated by the program. A brief explanation about

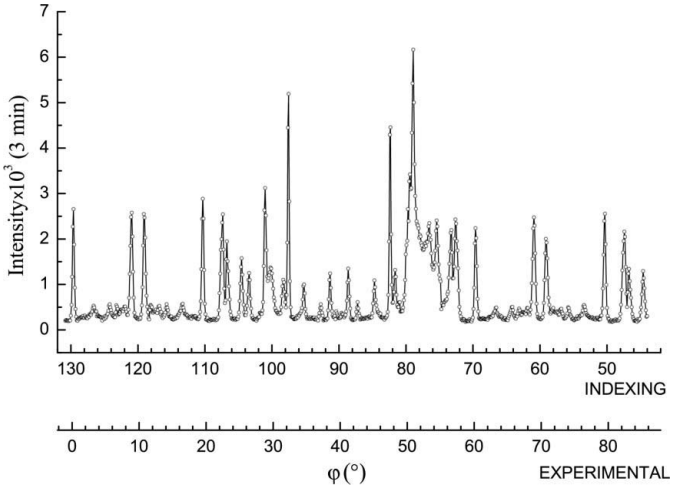

Figure 1
00.1 β-quartz NMD *Umweg* pattern measured at 1003 K by Mazzocchi (1984).

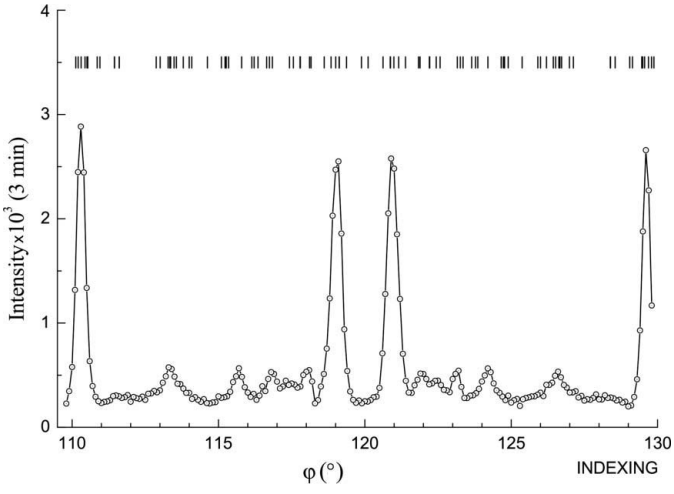

Figure 2
A small part of the experimental β-quartz pattern in an azimuthal angular interval extending from 109.5 to 130° on the indexing scale. The upper dashes are the result of the indexing process.

the absence of peaks in an experimental pattern will be given at the end of this section.

The variations of the φ positions as a function of parameter c for all pairs of secondary reflections occurring in the interval 115–120°, no matter if they give rise to experimental peaks or not, are shown in Fig. 3. We call the graph in Fig. 3 an 'indexing diagram' and the curves 'indexing curves'. The neutron wavelength used in the calculation was $\lambda = 1.1370$ Å. Actually, this wavelength was determined for the IPEN neutron diffractometer using a standard sample (Ni) and a procedure of calibration commonly employed at the time of the measurement of the β-quartz pattern (Parente *et al.*, 1967). It should be pointed out that this value, with an error (not specified) in the last decimal (10^{-4} Å), is also used in all other simulations in this work.

A comparison between Fig. 3 and the corresponding interval in Fig. 2 shows that the number of pairs in the indexing diagram is larger by a factor of ∼4.2 than that of experimental peaks. In other words, indexing shows a high density while the experimental pattern shows a low density of pairs. This was the first difficulty we found: how to correctly index the experimental pattern. This problem was solved by using the computer program *MULTI*, which was written to simulate NMD patterns of any type. This program was first used by Mazzocchi (1984) in the simulation of NMD patterns for the α and β phases of quartz. The results found for β-quartz were also reported by Mazzocchi & Parente (1994). In addition, Mazzocchi & Parente (1998) employed *MULTI* in the refinement of the ferri- and paramagnetic phases of magnetite.

To index the experimental pattern, we used a series of simulations of the 00.1 β-quartz NMD *Umweg* pattern. The simulated patterns, obtained with *MULTI*, were similar to those shown in Fig. 4. Each peak of the simulated patterns was fitted by a Gaussian in order to determine more precisely its φ position. The Gaussian fits were carried out by using the computer program *GAUSS* based on a least-squares method (Campos, 2002). Its output gives the φ positions of peaks accompanied by their uncertainties ($\varphi_i \pm \sigma_{\varphi i}$). Peaks having very low intensities were discarded. The φ positions found in all five simulations were plotted over Fig. 3. They correspond to the small circles that follow exactly some indexing curves. The pairs represented by such indexing curves are then responsible for the formation of the corresponding peaks in the simulated and experimental patterns. Five pairs were identified. All other pairs correspond to reflections permitted by the space group of β-quartz though producing no visible peaks in the pattern.

It should be noted that formation of a peak in an *Umweg* pattern depends on the coupling between one (or more) secondary beam and the primary beam (Chang, 1984). Pairs eliminated in the above process certainly correspond to those cases where the couplings are so weak that the resulting peaks have very low intensities or none at all. Another point to be noted is that parameter a, instead of c, could be used to find the pairs of relevant secondary reflections. As a matter of fact, Campos (2002) employed the procedure above taking c fixed and a varying. He obtained identical results to those of Fig. 3. This fact shows that the indexing of peaks is univocally determined irrespective of whether the value of a or of c is assumed fixed in the procedure.

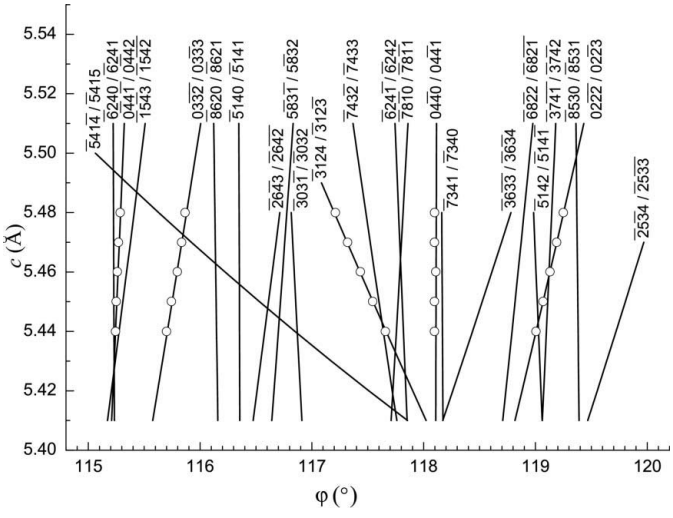

Figure 3
Indexing diagram as a function of c calculated with $a = 4.9977$ Å. Indexing curves were obtained for all pairs of permitted secondary reflections occurring in the interval 115–120°. Indexing curves showing superimpositions of small circles correspond to the correct indexing of both simulated and experimental patterns in the interval.

4. Classification of peaks

During data treatment we found that there are some peaks whose φ positions are more sensitive to the variation of one of the determined parameters than the other. A few peaks are equally sensitive to both parameters. The patterns in Fig. 4 are simulations obtained with *MULTI*. The pattern traced as a solid line was calculated using $a = 4.9977$ and $c = 5.4601$ Å (Wright & Lehmann, 1981). The pattern traced with a dashed line was calculated by conserving the value of c and changing

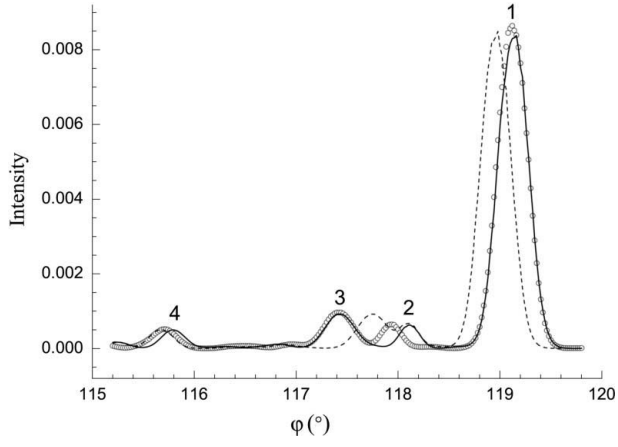

Figure 4
Simulated patterns calculated with $a = 4.9977$ and $c = 5.4601$ Å (solid line), $a = 4.9728$ and $c = 5.4601$ Å (small circles), and $a = 4.9977$ and $c = 5.4328$ Å (dashed line). The relative positions of the same peak in the three patterns show its sensitivity to variations of both a and c.

by ∼5% the value of *a*. The pattern represented by small circles was obtained by conserving the former *a* and changing by ∼5% the value of *c*. In Fig. 4 three types of peaks are shown. A comparison of the positions of the peaks of the dashed-line (d.l.) and small-circles (s.c.) patterns with the corresponding peaks of the solid-line pattern is done below. For the sake of clarity in the comparison, peaks in the solid-line pattern were numbered.

(*a*) In the s.c. pattern, the position of peak 1 does not change, at least in a perceptible way, while in the d.l. pattern it shifts approximately 0.2° to the left. This means that peak 1 is more sensitive to a variation of *c* than to a variation of *a*.

(*b*) Conversely, peak 2 is more sensitive to a variation of *a* than to a variation of *c*. Its position shifts ∼0.2° to the left in the s.c. pattern and remains practically unaltered in the d.l. pattern.

(*c*) The behaviour of peak 3 is identical to that of peak 1: it shifts approximately 0.4° to the right in the d.l. pattern. Because of this larger shift, it is certainly more sensitive to the variation of *c* than peak 1.

(*d*) Peak 4 is different from the first three: it is sensitive to both parameters, being slightly more sensitive to *c*.

If an experimental indexed peak in the NMD pattern had sufficiently high quality, *i.e.* if it had enough intensity and was isolated from its neighbours, it was selected as useful to be used in the determination of parameters. The selected peaks were then classified into two categories: those that are 'good for the determination of parameter *a*' (g.f.*a*) and those that are 'good for the determination of parameter *c*' (g.f.*c*).

Classification of peaks is done by first calculating the ratio

$$R = \Delta\varphi_a/\Delta\varphi_c, \qquad (1)$$

where $\Delta\varphi_a$ and $\Delta\varphi_c$ are angular shifts obtained from two (partial) indexing diagrams coexisting in the same graph.

Figs. 5 and 6 show how one can determine $\Delta\varphi_a$ and $\Delta\varphi_c$, respectively, for two different pairs of secondary reflections. In Fig. 5 the indexing curves were calculated by taking two fixed values of *c*. It should be noted that the indexing curves for the pair $04\bar{4}0/04\bar{4}1$ appear superimposed, while for the pair $02\bar{2}\bar{2}/02\bar{2}3$ they are clearly separated. An arbitrary value for *a* determines two values of $\Delta\varphi_a$. Owing to the separation of the indexing curves, $\Delta\varphi_a$ for the pair $04\bar{4}0/04\bar{4}1$ is negligible, while for the pair $02\bar{2}\bar{2}/02\bar{2}3$ it is ∼0.2°. Fig. 6 is equivalent to Fig. 5, except that the indexing curves were obtained by taking two fixed values for *a*. In Fig. 6 a reverse situation is observed: $\Delta\varphi_c$ for $04\bar{4}0/04\bar{4}1$ is about 0.2°, while for $02\bar{2}\bar{2}/02\bar{2}3$ it is negligible.

A comparison between the two figures leads to the conclusion that the φ position of the peak corresponding to the pair $04\bar{4}0/04\bar{4}1$ is very sensitive to a variation of *a* (Fig. 6) and almost insensitive to a variation of *c* (Fig. 5). For this reason, even when the value of *c* is assumed with a large error *a* can be determined with a quite good precision using such a peak: it is a g.f.*a* peak. Conversely, making a similar analysis, the peak corresponding to the pair $02\bar{2}\bar{2}/02\bar{2}3$ is a g.f.*c* peak. Calculating *R* for both peaks, in accordance with ratio (1) results in $R < 1$ for the g.f.*a* and $R > 1$ for the g.f.*c* peaks. Comparison of the value of *R* to one is then the criterion to be used in the classification of the selected peaks. It should be noted that the farther from one is the value of *R* the more precise is the determination of the corresponding parameter. It should also be noted that the case $R = 1$ seldom (or never) occurs. However, cases where the value of *R* is too close to one ($R \simeq 1$) occur, although less frequently. When $R \simeq 1$ the peak should be neglected in order to obtain a more precise determination of parameters. Taking this into account we have introduced an additional criterion: $R < 0.5$ for g.f.*a* and $R > 1.4$ for g.f.*c* peaks. This new criterion has been shown to be adequate for our purposes without severely diminishing the number of classified peaks. It should be mentioned that determination of the angular shifts $\Delta\varphi_a$ and $\Delta\varphi_c$ is carried out by taking values directly from the output of *INDEXHEX*, without actually plotting indexing diagrams.

Tables 1 and 2 list the g.f.*a* and g.f.*c* peaks, respectively, obtained from the experimental β-quartz NMD pattern and classified in accordance with the criterion given above. Peaks

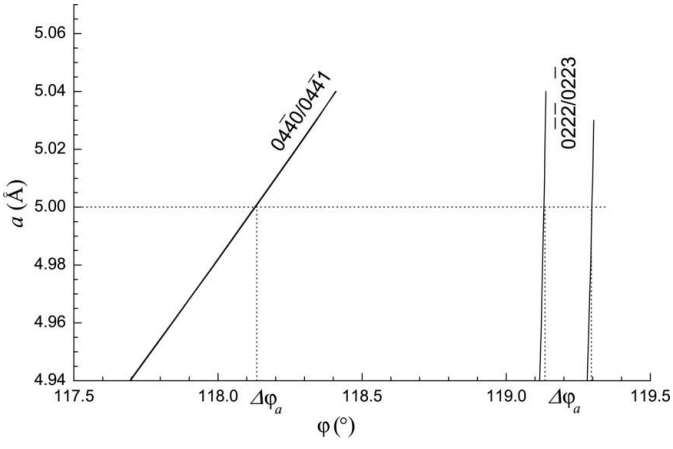

Figure 5
Determination of $\Delta\varphi_a$ for pairs $04\bar{4}0/04\bar{4}1$ and $02\bar{2}\bar{2}/02\bar{2}3$. Indexing curves were obtained by taking two fixed values of *c*, one assumed as +0.5% and other −0.5% of c = 5.4601 Å.

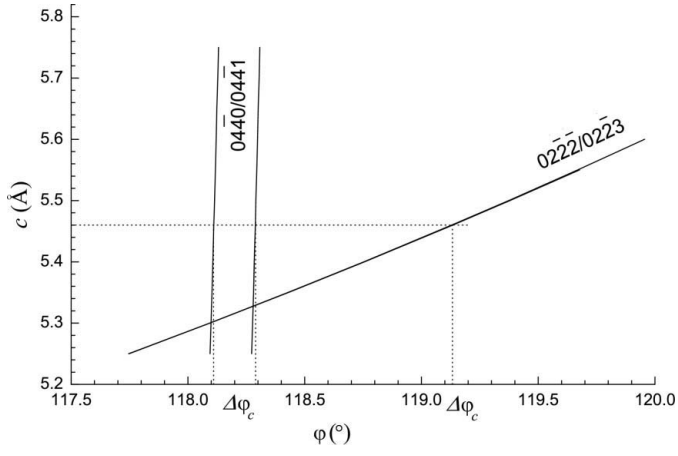

Figure 6
Determination of $\Delta\varphi_c$ for pairs $04\bar{4}0/04\bar{4}1$ and $02\bar{2}\bar{2}/02\bar{2}3$. Indexing curves were obtained by taking two fixed values of *a*, one assumed as +0.5% and other −0.5% of a = 4.9977 Å.

Table 1
Selected g.f.*a* peaks.

Peak *i*	Pair of secondary reflections	$\varphi_i \pm \sigma_{\varphi i}$ (°)	*R*
1	$\bar{3}4\bar{1}0/\bar{3}4\bar{1}1$	44.5789 ± 0.0196	0.01
2	$2\bar{1}\bar{1}0/2\bar{1}\bar{1}1$	46.7211 ± 0.0150	0.007
3	$4\bar{1}\bar{3}0/4\bar{1}\bar{3}1$	47.5731 ± 0.0181	0.01
4	$\bar{3}300/\bar{3}301$	53.3918 ± 0.0058	0.008
5	$\bar{3}30\bar{1}/\bar{3}302$	56.8306 ± 0.0053	0.38
6	$\bar{4}400/\bar{4}401$	61.8952 ± 0.0073	0.01
7	$30\bar{3}1/30\bar{3}2$	63.2187 ± 0.0031	0.34
8	$30\bar{3}0/30\bar{3}1$	66.6543 ± 0.0049	0.008
9	$\bar{4}310/\bar{4}311$	72.4308 ± 0.0194	0.01
10	$\bar{2}110/\bar{2}111$	73.2757 ± 0.0148	0.007
11	$\bar{5}41\bar{1}/\bar{5}412$	80.8279 ± 0.0025	0.14
12	$10\bar{1}0/10\bar{1}1$	82.4106 ± 0.0481	0.01
13	$21\bar{1}/2\bar{1}\bar{3}2$	84.7730 ± 0.0078	0.05
14	$\bar{4}220/\bar{4}221$	87.2301 ± 0.0065	0.01
15	$21\bar{3}0/21\bar{3}1$	88.6205 ± 0.0218	0.009
16	$\bar{3}120/\bar{3}121$	91.3652 ± 0.0090	0.009
17	$22\bar{4}0/22\bar{4}1$	92.7785 ± 0.0072	0.01
18	$\bar{3}12\bar{1}/\bar{3}122$	95.2763 ± 0.0062	0.05
19	$\bar{1}010/\bar{1}011$	97.5942 ± 0.0292	0.01
20	$05\bar{5}\bar{2}/05\bar{5}\bar{3}$	100.3751± 0.0118	0.37
21	$\bar{4}130/\bar{4}131$	104.5839 ± 0.0178	0.01
22	$11\bar{2}0/11\bar{2}1$	106.7142 ± 0.0151	0.07
23	$\bar{4}13\bar{1}/\bar{4}132$	107.5826 ± 0.0188	0.23
24	$\bar{3}030/\bar{3}031$	113.3711 ± 0.0050	0.008
25	$\bar{3}03\bar{1}/\bar{3}032$	116.7998 ± 0.0042	0.38
26	$04\bar{4}0/04\bar{4}1$	118.1139 ± 0.0093	0.01
27	$\bar{4}040/\bar{4}041$	121.8972 ± 0.0074	0.01
28	$03\bar{3}1/03\bar{3}2$	123.1635 ± 0.0055	0.38
29	$03\bar{3}0/03\bar{3}1$	126.6341 ± 0.0055	0.008

are identified by an integer i, $i = 1, 2, 3, \ldots, n$. The tables also list R and $\varphi_i \pm \sigma_{\varphi i}$ for each peak i.

5. Determination of parameters *a* and *c*

5.1. Procedure used in the determination of parameters

Fig. 7 is an indexing diagram calculated with c, $c + \sigma_c$ and $c - \sigma_c$ obtained from an experimental g.f.*c* peak i. It serves as an illustration in the procedure employed in the determination of parameter a with its uncertainty σ_a from all g.f.*a* peaks. In Fig. 7, for a position $\varphi_i \pm \sigma_{\varphi i}$ of a peak i, φ_i determines just one

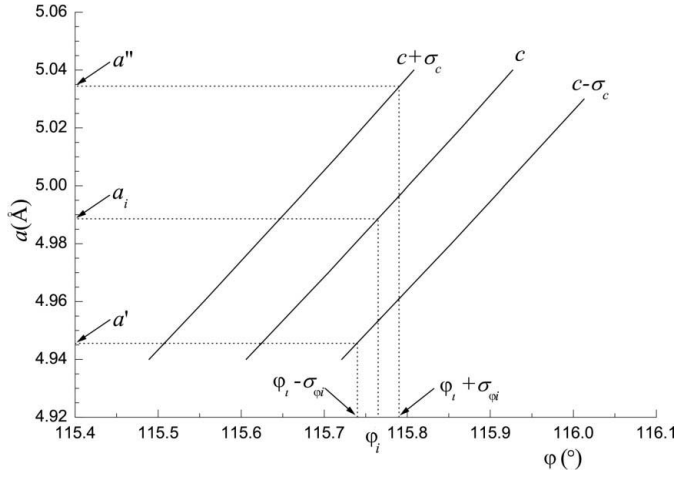

Figure 7
Determination of a_i, a' and a'' for an experimental g.f.*a* peak.

Table 2
Selected g.f.*c* peaks.

Peak *i*	Pair of secondary reflections	$\varphi_i \pm \sigma_{\varphi i}$ (°)	*R*
1	$30\bar{3}\bar{2}/30\bar{3}3$	55.7931 ± 0.0063	1.46
2	$20\bar{2}\bar{2}/20\bar{2}3$	59.1345 ± 0.0258	33.60
3	$\bar{2}20\bar{2}/\bar{2}203$	60.8759 ± 0.0241	33.60
4	$\bar{3}30\bar{2}/\bar{3}303$	64.2041 ± 0.0072	1.46
5	$\bar{3}21\bar{2}/\bar{3}213$	81.6280 ± 0.0075	2.39
6	$12\bar{3}\bar{2}/12\bar{3}3$	98.3731 ± 0.0133	2.36
7	$11\bar{2}1/11\bar{2}2$	101.0602 ± 0.0320	1.48
8	$\bar{3}12\bar{2}/\bar{3}123$	103.4024 ± 0.0120	2.36
9	$03\bar{3}\bar{2}/03\bar{3}3$	115.8012 ± 0.0079	1.46
10	$02\bar{2}\bar{2}/02\bar{2}3$	119.1351 ± 0.0271	33.60
11	$\bar{2}02\bar{2}/\bar{2}023$	120.8752 ± 0.0253	33.60
12	$\bar{3}03\bar{2}/\bar{3}033$	124.2057 ± 0.0065	1.46

value a_i. However, $\varphi_i - \sigma_{\varphi i}$ and $\varphi_i + \sigma_{\varphi i}$ determine four values resulting from the intersections of both angular positions with curves $c + \sigma_c$ and $c - \sigma_c$. We have chosen to represent $\varphi_i - \sigma_{\varphi i}$ and $\varphi_i + \sigma_{\varphi i}$, the smallest ($a'$) and the greatest ($a''$) values, respectively, below and above a_i.

In general, $|a'' - a_i|$ and $|a' - a_i|$ are slightly different. For this reason we have calculated a mean value for σ_{ai} given by expression (2) below:

$$s_{ai} = [|a'' - a_i| + |a' - a_i|]/2. \quad (2)$$

Finally, we obtain the result $a_i \pm \sigma_{ai}$ for a g.f.*a* peak i. An identical procedure can be employed in the determination of $c_i \pm \sigma_{ci}$, provided both a g.f.*c* peak i and a compatible indexing diagram are used.

The set of values $a_i \pm \sigma_{ai}$ obtained with all g.f.*a* peaks must be reduced to $a \pm \sigma_a$. In the same way $c_i \pm \sigma_{ci}$ must be reduced to $c \pm \sigma_c$. In this work, a and c were assumed as the weighted means of all a_i and c_i in the respective sets. Concerning the uncertainties for the means, σ_a and σ_c, it is worth paying attention to the statistical analysis of data described in §5.2.

Obviously calculated indexing curves are discontinuous, implying that interpolations often become necessary. We have used the program *INTERPOL* (Campos, 2002) to make linear interpolations when necessary. Another point is that, similarly to the determination of angular shifts $\Delta\varphi_a$ and $\Delta\varphi_c$, in the actual determination of parameters plotting of graphs becomes unnecessary.

5.2. Statistical analysis of data

The statistical analysis of an experimental data set can be carried out in several different ways. According to Woods (1990), special attention must be given to experimental details and uncertainties in the evaluation of an experimental data set. Purely mathematical analyses of experimental data should be viewed with caution. In this work, the criteria proposed by Chechev & Egorov (2000) were employed in the evaluation of data sets $a_i \pm \sigma_{ai}$ and $c_i \pm \sigma_{ci}$. According to these authors, the weighted mean and its uncertainty depend on the degree of data discrepancy of the experimental data. It can be quantified by comparing the χ^2 calculated for a given data set with both the degree of freedom ($n - 1$), where n is the number of experimental data, and the quantile of the χ^2 distribution

Table 3
Classification of data sets and recommended uncertainties (after Chechev & Egorov, 2000).

Classification of the data set	Type	Degree of data discrepancy (χ^2 value)	Recommended uncertainty (σ =)
Consistent	1	$\chi^2 \leq (n-1)$	σ_w
Slightly discrepant	2	$(n-1) < \chi^2 \leq (\chi^2)^{0.05}_{n-1}$	$\sigma_w\,[\chi^2/(n-1)]^{1/2}$
Discrepant	3	$(\chi^2)^{0.05}_{n-1} < \chi^2 \leq 10(\chi^2)^{0.05}_{n-1}$	$\sigma_w\,[\chi^2/(n-2)]^{1/2}$
Discrepant	4	$\chi^2 > 10(\chi^2)^{0.05}_{n-1}$	$\sigma_w\,[\chi^2/(n-3)]^{1/2}$

calculated at a significance level of 0.05, *i.e.* $(\chi^2)^{0.05}_{n-1}$. The value of χ^2 is calculated by using the expression

$$\chi^2 = \sum[(x_i - x_m)^2/\sigma_i^2], \quad (3)$$

where x_i and σ_i refer, respectively, to the individual values in the data set and their uncertainties and x_m is the weighted mean calculated by the expression

$$x_m = \sum(x_i/\sigma_i^2)/\sum(1/\sigma_i^2). \quad (4)$$

Four types of data sets can be defined according to the degree of data discrepancy. For each one, Chechev & Egorov (2000) recommended an uncertainty σ to be associated with the weighted mean x_m. Classification of the data sets together with the recommended uncertainties is given in Table 3.

In Table 3, σ_w is the standard deviation of the weighted mean (internal error), which is given by

$$\sigma_w = \left[1/\sum(1/\sigma_i^2)\right]^{1/2}. \quad (5)$$

5.3. Determination of parameters using an iterative process

We soon realized that the determination of parameters in the way described in §5.1 would be better accomplished if an iterative process was used. Iteration would certainly improve the accuracy of the determination. To start the iterative process, a was arbitrarily chosen as the first parameter to be determined in the first cycle of the process. For this first determination a fixed value for c was intentionally assumed equal to 5.500 Å (without an uncertainty), in order to obtain a better and clearer picture of how a parameter converges in the process of iteration. With the above value of c a set of values $a_i \pm \sigma_{ai}$ was determined using positions $\varphi_i \pm \sigma_{\varphi i}$ in Table 1. Of course, no $c + \sigma_c$ and $c - \sigma_c$ were used this time. To continue the first cycle the set $a_i \pm \sigma_{ai}$ must be reduced to $a \pm \sigma_a$ in order to determine $c \pm \sigma_c$. This reduction was obtained by calculating the weighted mean using expression (4) and taking into account Table 3. This resulted in $a \pm \sigma_a$ = 4.9904 ± 0.0012 Å.

To finish the first cycle, a, $a + \sigma_a$ and $a - \sigma_a$ were taken as fixed values and a set $c_i \pm \sigma_{ci}$ was then determined using the g.f.c peaks of Table 2. The set was reduced to $c \pm \sigma_c$ = 5.46548 ± 0.00043 Å. The iterative process continued until both $a \pm \sigma_a$ and $c \pm \sigma_c$ converged, each one to a value that was assumed as the final value for the corresponding parameter. It should be noted that, in the determination of uncertainties σ_a and σ_c, we used expressions (3) and (4) to calculate χ_a^2 and χ_b^2 for each cycle of iteration. With χ_a^2 and χ_b^2, expression (5), and Table 3, we could calculate the uncertainties and classify sets $a_i \pm \sigma_{ai}$ and $c_i \pm \sigma_{ci}$ as well. Fig. 8 shows examples of application of the statistical analysis of the data. The data sets plotted in Fig. 8 were obtained in the second cycle of the iterative process. It is worth noting that, no matter what the cycle is, sets $a_i \pm \sigma_{ai}$ and $c_i \pm \sigma_{ci}$ always behave like those appearing in Fig. 8.

Table 4
Values of $a \pm \sigma_a$ and $c \pm \sigma_c$ found in 12 cycles of the iterative process.

Cycle No.	χ_a^2	χ_c^2	$a \pm \sigma_a$ (Å)	$c \pm \sigma_c$ (Å)
1	1025.556	11.918	4.9904 ± 0.0012	5.46548 ± 0.00043
2	1216.401	7.409	4.9953 ± 0.0014	5.46222 ± 0.00039
3	1416.349	7.831	4.9977 ± 0.0017	5.46024 ± 0.00026
4	1169.129	5.580	4.9960 ± 0.0014	5.46162 ± 0.00035
5	1072.770	6.050	4.9958 ± 0.0014	5.46165 ± 0.00034
6	1220.012	6.119	4.9961 ± 0.0015	5.46145 ± 0.00034
7	1071.231	5.203	4.9955 ± 0.0014	5.46192 ± 0.00041
8	1289.080	4.239	4.9959 ± 0.0015	5.46187 ± 0.00033
9	1218.450	5.786	4.9956 ± 0.0014	5.46184 ± 0.00035
10	1244.111	5.778	4.9957 ± 0.0014	5.46184 ± 0.00035
11	1244.111	5.778	4.9957 ± 0.0014	5.46184 ± 0.00035
12	1244.111	5.778	4.9957 ± 0.0014	5.46184 ± 0.00035

6. Final results and comments

Table 4 lists the results obtained in 12 cycles of the iterative process. This table also includes χ_a^2 and χ_c^2 calculated, respectively, for sets $a_i \pm \sigma_{ai}$ and $c_i \pm \sigma_{ci}$ in each cycle.

It is important to observe that for parameter a the convergence occurred from the tenth cycle on, with a precision of the order of 10^{-3} Å, and for parameter c from the ninth

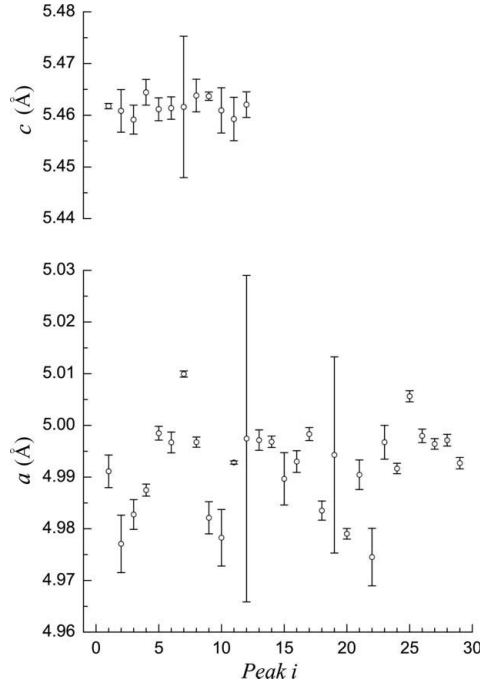

Figure 8
Plots of peak i *versus* $a_i \pm \sigma_{ai}$ (below) and peak i *versus* $c_i \pm \sigma_{ci}$ for data sets obtained in the second cycle of the iterative process. The set $a_i \pm \sigma_{ai}$ was classified as type 4 – discrepant – and $c_i \pm \sigma_{ci}$ as type 1 – consistent.

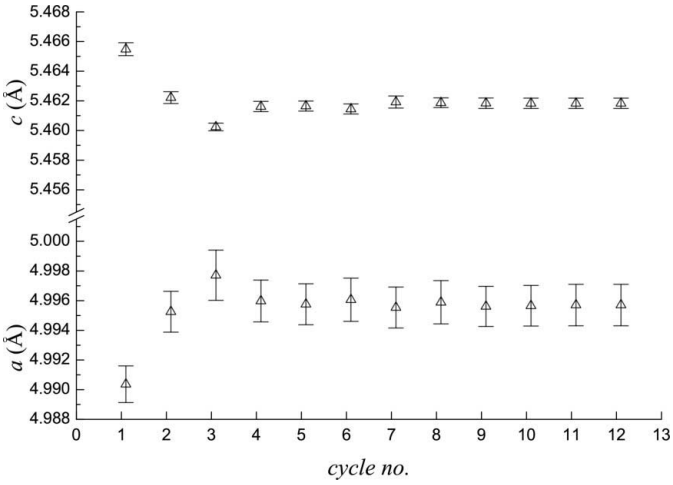

Figure 9
Plot showing the convergences of $a \pm \sigma_a$ and $c \pm \sigma_c$ in the 12 cycles performed.

cycle on, with a precision of the order of 10^{-4} Å. The difference in precision between *a* and *c* is probably due to the fact that data sets obtained with g.f.*a* peaks are discrepant while those obtained with g.f.*c* peaks are consistent. They differ by approximately one order of magnitude, even for a case where the number of g.f.*a* peaks ($n = 29$) is ∼2.4 times that of g.f.*c* peaks ($n = 12$). The results obtained after the convergence, namely $a \pm \sigma_a = 4.9957 \pm 0.0014$ and $c \pm \sigma_c = 5.46184 \pm 0.00035$ Å, were assumed as the final values for the hexagonal cell parameters of β-quartz at 1003 K.

Fig. 9 is a plot of cycle number *versus* both $a \pm \sigma_a$ and $c \pm \sigma_c$ as listed in Table 4. It shows clearly how the convergence occurs in the iterative process.

The procedures developed in this work can be defined as a nondestructive single-crystal method. As such it is useful for those people who need to obtain the lattice parameters of a single crystal from a simple experiment without destroying the sample. Measurement of a multiple diffraction pattern is easily carried out. After a careful orientation of the single crystal to obtain the primary reflection, the measurement is reduced to a simple rotation around the scattering vector of the primary reflection (φ scan). In what follows, a few remarks are made on the application of the technique to unit-cell parameter determination.

(*a*) Mazzocchi & Parente (1998) discussed application of NMD in structural analysis. Most of their observations could also be applied to the determination of unit-cell parameters.

(*b*) The experimental NMD pattern used in this work was limited to ∼87°. In a full (360°) pattern of the same compound the number of peaks would be greater accordingly. With a greater number of peaks, more restrictive values for *R* can be assumed, increasing the precision in the results. In general, to measure a full pattern is only a matter of extending the duration of the experiment.

(*c*) For a given sample, several different patterns measured with different primary reflections can be used. This allows the employment of a wide variety of peaks to assess their sensitivities to the parameters. In principle, no new crystal orientation is necessary.

(*d*) The methodology developed in this work is not limited to the use of neutrons. X rays from standard or synchrotron sources can also be used, generally with advantages concerning the intensity and divergence of the monochromatic beam and the precision in the knowledge of the wavelength.

(*e*) Procedures other than those developed in this work could be used to attain the same objectives. This is also the case of the computer programs used in the procedures. For example programs *UMWEG* (Rossmanith, 1985, 2003*a*, 2006, 2007) and *PSILAM* (Rossmanith, 2003*b*) could be used instead of *MULTI* and *INDEXHEX*, respectively.

The authors are indebted to Professor O. Helene, from Instituto de Física da Universidade de São Paulo, Brazil, for both advice and fruitful discussions concerning the statistical analysis of data. LCC acknowledges the Pontifícia Universidade Católica de São Paulo, Brazil, for a CEPE fellowship.

References

Campos, L. C. (2002). PhD thesis, Universidade de São Paulo, SP, Brazil.
Cardoso, L. P. (1983). PhD thesis, Universidade Estadual de Campinas, SP, Brazil.
Caticha-Ellis, S. (1975). *J. Appl. Phys.* **14**, 603–612.
Chang, S.-L. (1984). *Multiple Diffraction of X-rays in Crystals.* Berlin, Heidelberg, New York, Tokyo: Springer-Verlag.
Chechev, V. P. & Egorov, A. G. (2000). *Appl. Rad. Isot.* **52**, 601–608.
Cole, H., Chambers, F. H. & Dunn, H. M. (1962). *Acta Cryst.* **15**, 138–144.
Dana, J. D. & Dana, E. S. (1962). *The System of Mineralogy*, Vol. 3, *Silica Minerals*. New York: Wiley.
Kossel, W. (1936). *Ann. Phys.* (*Leipzig*), **25**, 512. **[Final page?]**
Mazzocchi, V. L. (1984). MSc dissertation, Universidade de São Paulo, SP, Brazil.
Mazzocchi, V. L. & Parente, C. B. R. (1994). *J. Appl. Cryst.* **27**, 475–481.
Mazzocchi, V. L. & Parente, C. B. R. (1998). *J. Appl. Cryst.* **31**, 718–725.
Parente, C. B. R. & Caticha-Ellis, S. (1974). *Jpn. J. Appl. Phys.* **13**, 1506–1513.
Parente, C. B. R., Harada, K., Koishi, Y. & Wenzel, R. G. (1967). *Publ. IEA*, **152**, 121–124a.
Post, B. (1975). *J. Appl. Phys.* **8**, 452–456.
Renninger, M. (1937). *Z. Phys.* **106**, 141–176.
Rossmanith, E. (1985). *Z. Kristallogr.* **171**, 253–254.
Rossmanith, E. (2003*a*). *J. Appl. Cryst.* **36**, 1467–1474.
Rossmanith, E. (2003*b*). *J. Appl. Cryst.* **36**, 1098–1100.
Rossmanith, E. (2006). *Acta Cryst.* A**62**, 174–177.
Rossmanith, E. (2007). *Acta Cryst.* A**63**, 251–256.
Woods, M. J. (1990). *Nucl. Instrum. Methods Phys. Res. Sect. A*, **286**, 576–583.
Wright, A. F. & Lehmann, M. S. (1981). *J. Solid State Chem.* **36**, 371–380.